

Model for a steam methane reforming reactor with metal foam catalyst substrate

B. Saberi, S. Saberi¹, D. Naumann², W. Doelling³

Green Twirl Energy Ltd., 427 Dorland Rd., Oakville, ON L6J 6B3, Canada;

tel: +1 416 278 8543, email: babak@greentwirlenergy.com

¹S. Saberi, Consultant, 427 Dorland Rd., Oakville, ON L6J 6B3, Canada;

tel: +1 289 218 7533, email: ssaberi@cogeco.ca

²Juniper Associates Ltd., 5439 Middlebury Drive, Mississauga, ON L5M 5E8,

Canada; tel: +1 647 393 6783, email: dnaumann@rogers.com

³Alantum Europe GmbH, Lyonel-Feininger-Str. 28, 80807 Munich, Germany;

tel +49 89 729 49 49 49, email: wdoelling@alantum.com.

Abstract

Metallic foams are structured porous substrates that can be used as catalyst support with superior heat transfer and mass transfer due to their enhanced flow mixing, large surface area and optimal thermal properties. They have the potential of replacing conventional pellets or packing material in a range of applications in chemical industry, e.g. catalytic reforming, hydrogen production, distillation, micro-reactors, compact heat exchangers and static mixers.

Certain categories of metallic foams can be made to possess a homogeneous and reproducible morphology, particularly suitable for catalyst substrates. The open porous structure and thin struts of these foams minimize the blocking of the pores during the coating process which leads to lower pressure drop in comparison with other metallic and ceramic foams. It is expected that the enhanced mass and heat transfer rates with these foams used as catalyst substrates result in significantly reduced physical and energy footprints in a large number of packed bed processes.

At the present time, there is a strong interest in the chemical and alternative energy industrial sectors in testing and evaluation of metallic foams in comparison with conventional pellets for the process of Steam Methane Reforming (SMR) and similar gas-phase reaction systems such as methanol synthesis. Developing a theoretical model that could serve as a mean to provide more in depth understanding of the performance of alloy foams in such systems and to assess their relative performance in comparison with traditional packed bed is vital in the process of benchmarking and application development.

The present work consists of the development of a theoretical model for a wall-heated tubular SMR metallic foam reactor including reaction kinetics, pore diffusion, mass transfer and heat transfer. The enhanced mixing is modeled by considering the flow-structure interactions through the application of a modified turbulence model. The computational fluid dynamics (CFD) is used to solve the model equations. The model is calibrated with available literature data and a final quantitative model within an acceptable margin that is robust within the range of operating parameters of interest. The performance of the foam bed is compared with a pellet bed for a number of operating conditions pertinent to the SMR system. The results include reactor yield and selectivity, temperature profiles and pressure drop. It is demonstrated that such model can constitute a robust tool for design and optimization of foam bed reactors.

Introduction

Catalytic packed bed reactors are at the heart of many chemical and petrochemical processes. These reactors are typically filled with catalyst pellets such as cylindrical, extruded, or other shapes. In highly endothermic or exothermic reactions where heat needs to be transferred to or from the bed through its walls, a single packed bed is not a satisfactory choice. In such systems, a multi-tube configuration could be preferred to provide a large heat transfer surface area. In addition to a large external area, good internal heat transfer properties are essential to avoid large thermal gradients, and maximize the efficiency of the reaction. Alternative high porosity structures that are durable and can be coated with catalyst (washcoat), could be more energy efficient choices over pellet beds. Examples of such structures are ceramic and metallic foams and monoliths.

Open cell metallic foams are highly porous substrates that can be used as catalyst support with superior heat transfer and mass transfer due to their enhanced flow mixing, large surface area and optimal thermal properties. They are produced in a variety of pore sizes and compositions, and have the potential of replacing conventional pellets or packing material in a range of applications in chemical industry, e.g. catalytic reforming, hydrogen production, distillation, micro-reactors, compact heat exchangers and static mixers.

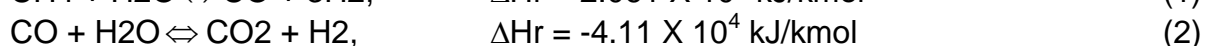
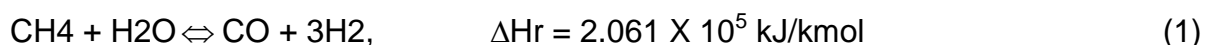
In order for such applications to be implemented effectively and successfully, it is important to acquire a theoretical understanding of how such novel structures can perform in comparison with conventional packings. There are numerous studies published on flow, heat and mass transfer properties of catalytic packed beds, however, few studies offer a quantitative assessment of the performance of these alternative catalyst supports.

The present work describes a macro-scale Computational Fluid Dynamics (CFD) model developed to assess the performance of metallic foam catalyst substrates in comparison with the conventional pellet catalysts in the Steam Methane Reforming (SMR) process. The SMR process with its highly endothermic behavior was selected as a suitable case for this study.

The SMR Process

Steam reforming of natural gas is the most important and economic process for production of hydrogen and synthesis gas needed in many chemical and petrochemical processes. The steam reformer is a furnace containing burners and tubes packed with nickel catalyst on porous alumina support.

The following important reactions take place within the reformer:



(3)

The reforming reactions (1) and (3) occur (in parallel) primarily in the steam reformer while thermodynamics favor higher conversions of the shift reaction (2) in the shift reactors.

Heat Transfer Limitation

Due to the strongly endothermic nature of reactions (1) and (3), a large amount of heat is supplied by fuel burning (commonly natural gas) in the furnace chamber, making the process heat transfer-limited. Due to the high heat input through the reformer tube wall and the endothermic reforming reactions, the catalyst tubes are exposed to significant axial and radial temperature gradients. For side fired reformers, axial temperature differences around 200-270°C and radial temperature gradients up to 80°C have been reported. The tube wall material should be durable enough to sustain this high thermal load, combined with large temperature gradients. It is common knowledge that even a slight increase in the maximum tube wall temperature may result in a serious decline of the expected tube lifetime.

Heat transfer is facilitated by using multiple long reactor tubes of small diameter to give the necessary heat transfer surface. As pointed out by Twigg and Richardson (Twigg and Richardson, 2007), the consequence of having long narrow tubes could be a significant pressure drop penalty. Making the pellets larger can reduce pressure drop, and although this increases radial heat transfer, the effectiveness factor decreases and more catalyst volume is then required.

Ceramic and metallic foams used as catalyst substrate can relieve all these problems. Metallic foams for their high thermal conductivity, high porosity, light weight, shapability, low pressure drop, and desirable flow mixing characteristics are of particular interest.

Open Cell Metal Foams as Catalyst Substrate

Open cell metal foams typically have good homogeneity and can be tailored to have excellent oxidation- and corrosion-resistance, and superior mechanical properties, which open up a series of potential new applications as heat exchange media, micro-mixers, and catalysis. The metal usually consists of an alloy with a composition optimized to fit the chemical process environment.

The consistency of the foam microstructure is, to a large degree, a function of the manufacturing process. One process especially suitable for producing small pore size foams with a high percentage of open cells and structural uniformity uses a nickel foam precursor made from electrolytic deposition of nickel on polyurethane foam, followed by heat treatment. (Walther et al., 2008). The nickel foam is continuously unwound, coated first with a binder solution using an immersion or spraying process and then with a specified metal powder, after which it is cut into sheets of the desired size before heat-treating. During the subsequent sintering step, the final composition of the foam and its specific surface area and porosity can be adjusted as desired (Figure 1). Diffusion rates are enhanced through transient liquid phase sintering, allowing for rapid homogenization. The process also allows for the coating of the base substrate with multi-phase composite powders and is hence also suitable for manufacturing complex alloy compositions.

Due to the manufacturing procedure, the foams exhibit no blocked pores and their geometry follows with accuracy the original polyurethane foam geometry, as shown in Figure 2. The open porous structure and thin struts of these foams minimize the blocking of the pores during the coating process which leads to lower pressure drop in comparison with other metallic and ceramic foams.

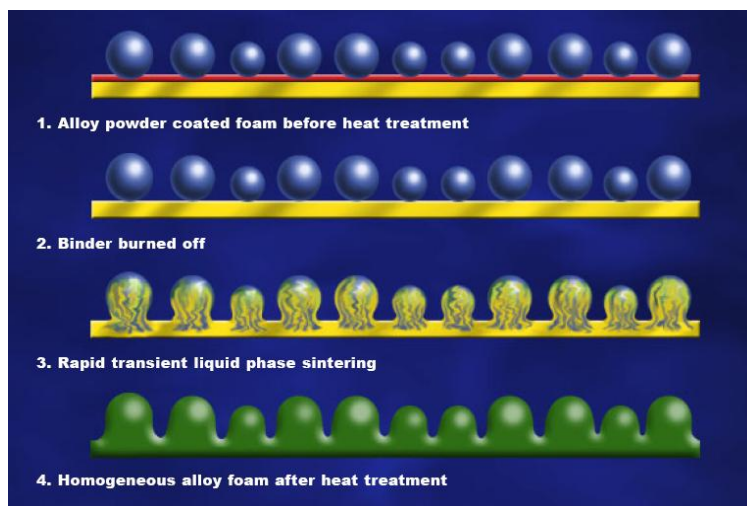


Figure 1. Schematic illustration of processes occurring during transient liquid phase sintering with increasing temperature/time

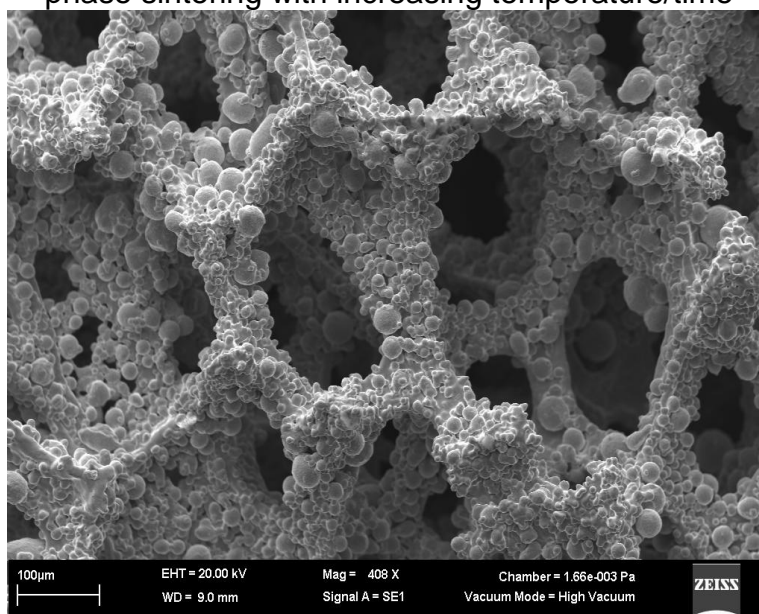


Figure 2. SEM-picture of an Inconel foam from nickel foam precursor

At the present time, there is a strong industrial interest in testing and evaluation of metallic foams in comparison with conventional pellets for the SMR process and similar gas-phase reaction systems such as methanol synthesis. The potential advantages associated with the use of metal foams as SMR catalyst need a quantitative assessment of how such foams perform in comparison with pellets. This can be achieved through the development of a theoretical model based on fundamental mass, momentum, and energy conservation. CFD is a particularly suitable platform to develop such model, which has an inherently significant degree of non-linearity and coupling.

The Present Work

1-D, 2-D and 3-D mathematical models describing flow, reaction and heat transfer in SMR reactors made of conventional pellets have been developed and published extensively. Examples of such models are found in Hyman (1968), Xu and Froment (1989), Ferreira et al. (1992), Kvamsdal et al. (1999), Grenvskott et al. (2001),

Pedernera et al. (2003), Kirillov et al. (2003), El-Bousiffia (2007), Dixon et al. (2007), Sadeghi and Molaei (2008), and de Jong et al. (2009).

Heat and mass transfer properties of metallic and ceramic foams has been also studied for packed bed applications, for example by Giani et al. (2005), and Zhao et al. (2004) and (2005). However, models for catalyzed metal foams including flow, heat transfer and reaction have not been developed to the same extent as that of pellet beds for the SMR process.

The primary objectives of this work were the following:

- Develop a mathematical model for a SMR pellet reactor and validate the model
- Study and demonstrate the heat transfer characteristics of metal foams as SMR catalyst substrate in comparison with pellet catalyst through simulations using the developed model. Some preliminary optimization scenarios were also simulated to demonstrate that the model could be used to determine operating conditions that could improve the SMR reactor operability and productivity.

The model was validated against available data from literature in order to create a final quantitative model with an acceptable accuracy and robustness within the range of operating parameters of interest. The performance of the foam and pellet beds was compared for a number of operating conditions pertinent to the SMR system.

SMR Reactor Model

This section describes the fundamental CFD model assumptions, equations and input parameters.

Model Assumptions and Equations

The model was developed for the steady flow of a gas mixture through a bed made of pellets or foam defined as a porous material with a given porosity and resistance to the flow. This flow resistance results in a pressure drop across the catalyst tube. The gaseous species are transferred from the bulk of the gas through mass transfer, diffuse in the porous catalyst support and reach the catalyst active surface. As a result of endothermic reaction, the catalyst is subject to large temperature gradients. A two-phase heat transfer model approach was used to reflect the fact that the catalyst and gas could have different temperatures. The simulation domain consisted of one heated-wall tube. Assuming symmetry in the azimuthal direction, a 1/16 slice of the cross section was considered.

The mass transfer resistance due to diffusion of species in catalyst pores was considered by applying an effectiveness factor. This factor reflects the fact that under such conditions, the concentration of the reacting species at the active surface of the catalyst is less than that of the bulk gas. The effectiveness factors were taken from Xu and Froment (1989).

The heat transfer model included convection, conduction and radiation mechanisms. The radiation effect was included by combining the foam material thermal conductivity with an equivalent radiation thermal conductivity. It should be noted that while most of the work of thermal conductivity of metallic foams have used an overall gas + solid thermal conductivity, the two-phase flow model used in the present work requires separate gas and solid effective thermal conductivities. Therefore, effect of gas phase mixing was introduced in the gas-phase thermal conductivity, and the effect of solid-solid and wall-solid radiation was included in the solid-phase as an enhanced solid thermal conductivity. An approximate equivalent

solid thermal conductivity was derived from the literature (Zhao et al. 2004 and 2005).

A gas-phase mixing model for the foam substrate provided the basis for heat and mass transfer between the bulk of the gas phase and the surface of the foam. The mixing model consists of two main components:

1. A turbulence model that describes the additional mixing effects due to flow disturbances due to the presence of the solid phase (pellet or foam catalyst). A simple mixing length approach was used to relate the morphology of the solid substrate to gas phase turbulence.
2. A heat/mass transfer model that determines the rate of exchange of heat and mass transfer at the gas-solid interface.

Table 1 gives the model conservation equations for the gas and solid phases based on the assumptions made above. The terms and symbols used in the equations are described in the nomenclature.

Figure 3 illustrates the inside wall boundary temperature. A wall heat transfer coefficient relates this temperature to the gas temperature in the vicinity of the wall across the boundary layer. Correlations given by Peters et al (1988) and Zhao et al. (2001) are used respectively for cylindrical pellets and metal foams.

SMR kinetics

The Xu & Froment model for SMR kinetics as described in “Methane Steam Reforming, Methanation and Water-Gas Shift – Parts I & II”, AIChE Journal (1989) was used to calculate the reactions rates (Eqs. 4-8). The kinetic and adsorption parameters for the SMR system from Xu and Froment are given in Tables 2 and 3.

Table 1. Model governing equations

Gas Phase	
Continuity	$\nabla \cdot (\rho U) = 0$
Momentum	$\nabla \cdot (\rho U \otimes U) = -\nabla P + \nabla \cdot \tau + S_M$
Energy	$\nabla \cdot (\rho U h_{tot}) = \nabla \cdot (\lambda \nabla T) + \nabla \cdot (U \cdot \tau) + U \cdot S_M + h_{sg} a_{sg} (T - T_s)$
Species Mass Fractions	$\frac{\partial (\rho U_j Y_i)}{\partial x_j} = \frac{\partial}{\partial x_j} \left(D_{i,eff} \frac{\partial Y_i}{\partial x_j} \right) + S_i$
Turbulence	$\mu_t = \rho \alpha f_u U_t l_t$
Pressure Drop	$-\frac{\partial P}{\partial x_i} = \frac{\mu}{K_{perm}} U_i + K_{loss} \frac{\rho}{2} U U_i$
Solid Phase	
Solid Temperature	$\nabla \cdot (\lambda_s \nabla T_s) + h_{sg} a_{sg} (T - T_s) = \sum_{j=1}^3 \rho_s r_j \Delta H_j$
Gas-Solid Interface	
Heat Transfer	$Nu = A Re^{0.42} Pr^{0.33}$

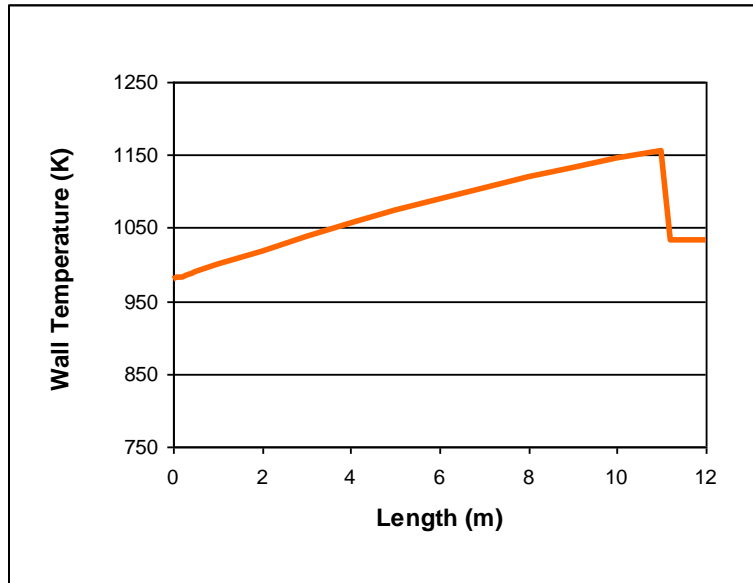


Figure 3. Inside wall temperature profile

$$r_1 = \frac{k_1}{P_{H_2}^{2.5}} (P_{CH_4} P_{H_2O} - \frac{P_{H_2}^3 P_{CO}}{K1}) / (DEN)^2 \quad (4)$$

$$r_2 = \frac{k_2}{P_{H_2}} (P_{CO} P_{H_2O} - \frac{P_{H_2} P_{CO_2}}{K2}) / (DEN)^2 \quad (5)$$

$$r_3 = \frac{k_3}{P_{H_2}^{3.5}} (P_{CH_4} P_{H_2O}^3 - \frac{P_{H_2}^3 P_{CO_2}}{K3}) / (DEN)^2 \quad (6)$$

$$DEN = 1 + K_{CO} P_{CO} + K_{H_2} P_{H_2} + K_{CH_4} P_{CH_4} + K_{H_2O} P_{H_2O} / P_{H_2} \quad (7)$$

$$k_i = A_i \exp\left(\frac{-E_i}{RT_{solid}}\right) \quad (8)$$

$$j = CO, H_2, CH_4, H_2O$$

Table 2. SMR reactions rate parameters

Reaction Number	$A_i, \text{ kmol} \cdot \text{bar}^{0.5} \cdot \text{kg}_{\text{cat}}^{-1} \cdot \text{h}^{-1}$	$E_i, \text{ kJ/mol}$
1	4.225×10^{15}	240.1
2	1.955×10^6	67.13
3	1.020×10^{15}	243.9

Table 3. Parameters for the adsorption different species on the catalyst surface

Species	$A_j, \text{ bar}^{-1}$	$\Delta H_j, \text{ kJ} \cdot \text{mol}^{-1}$
CO	1	-70.65
H ₂	2	-82.9
H ₂ O	3	-38.28
CH ₄	4	88.68

Input Parameters

The input parameters to the CFD model are summarized in tables 4-6 below.

Table 4. Reactor tube characteristics

Tube length (m)	12
Heated tube length (m)	11.1
Tube outside diameter (m)	0.132
Tube inside diameter (m)	0.101

Table 5. Inlet temperature, pressure and flow rate

Inlet temperature (K)	793.15
Inlet pressure (bar)	29
Natural gas flowrate per tube (Nm ³ /h)	135.00
Steam flowrate per tube (Nm ³ /h)	399.17

Table 6. Species feed rate (kmol/h)

Species	kmol/h
CH ₄	5.168
H ₂ O	17.354
CO ₂	0.289
H ₂	0.630
N ₂	0.847
CO	0.0

The characteristics of the cylindrical pellets are given in Table 7.

Table 7. Pellet catalyst properties

Outer diameter (m)	0.0173
Inner diameter (m)	0.0084
Height (m)	0.010
Thickness of active layer (m)	0.002
Density (kg/m ³)	2355
Pellet Void fraction (-)	0.45
Specific heat (kJ/K/kmol)	1000
Thermal conductivity (W/K/m)	4.6

CFD Solution

The model geometry was constructed and meshed using the meshing software ICEM CFD HEXA from ANSYS. The computational hexahedral mesh is shown in Figure 4. The mesh was transferred into the CFD solver ANSYS-CFX and the problem was set up using the above input parameters. The solver was run until the residual errors of all of the conservation equations fell below 10⁻⁶.

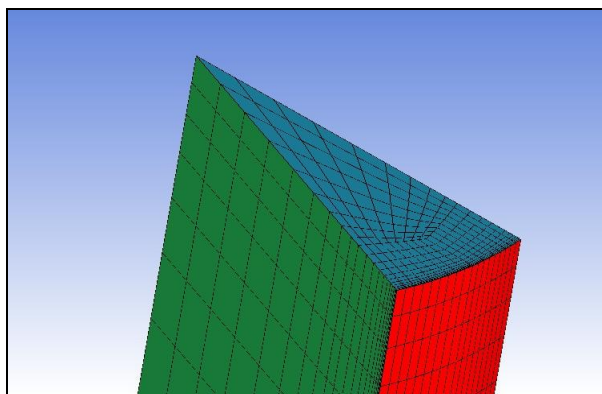


Figure 4. The computational domain of the SMR reactor tube

Results

The CFD results are explained in the next subsections. First, the results for a pellet bed are illustrated and compared with data provided by Xu and Froment (1989). Then, the results obtained for a foam bed operating in similar conditions are presented. Finally, a parametric study is performed to examine how foam catalyst can provide advantages over the pellet catalyst.

Pellet Bed Reactor Model Results and Validation

Figures 5 and 6 show the CFD model results for the pellet bed in the form of radially averaged gas temperature and methane mole fraction profiles along the vertical axis of the bed. As can be observed, the CFD model shows satisfactory agreement with model results given by Xu and Froment. Figure 7 compares the gas and solid temperature profiles along the bed, which indicates that temperature of the pellets is typically about 15 °C lower than that of the gas.

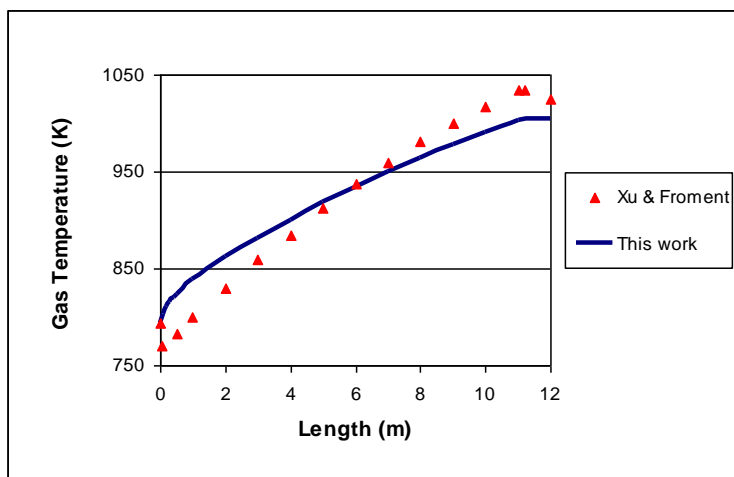


Figure 5. Axial profile of radially averaged gas temperature in the pellet bed

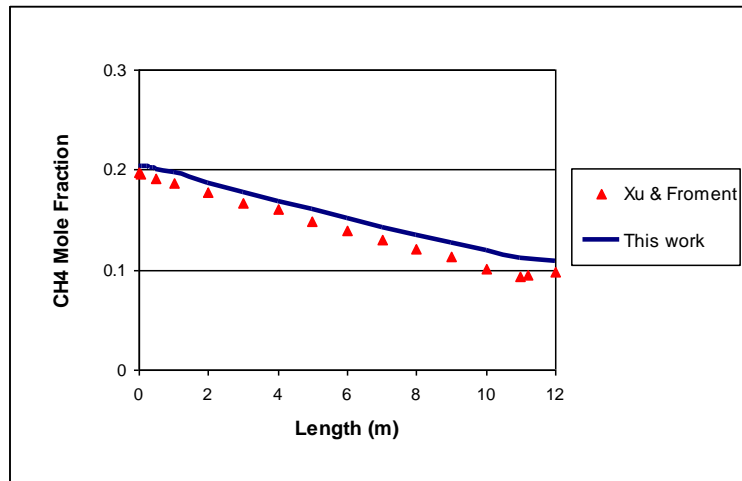


Figure 6. Axial profile of radially averaged methane mole fraction in the pellet bed

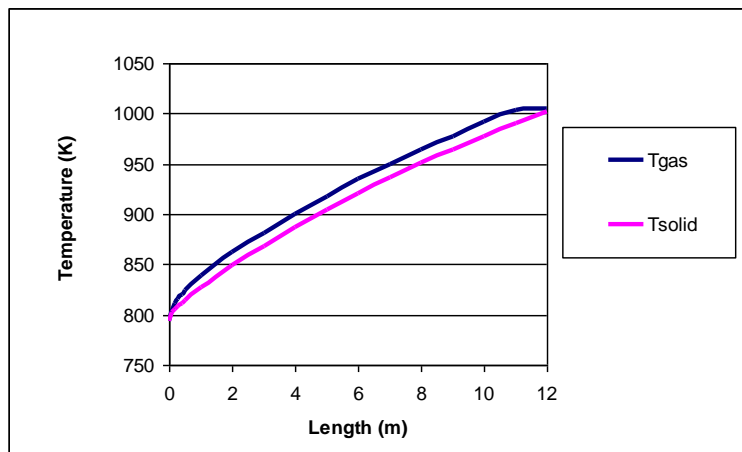


Figure 7. Axial profiles of radially averaged gas and solid temperatures in the pellet bed

Foam Bed Reactor Model Results

A similar model was developed for a bed consisting of a FeCrAlloy foam with 1200 micron nominal cell size. The morphological and thermal properties of this foam are given in Table 8. A washcoat thickness of 15 micron was considered to be deposited on the foam. It was assumed that one kilogram of this washcoat had an intrinsic activity similar to one kilogram of pellet catalyst. Therefore, the total amount of the catalyst used in the foam bed was equal to approximately half of the catalyst used in the pellet bed. At this order of magnitude of catalyst thickness, it is well known that the pore diffusion is minimal and therefore the effectiveness factors were considered to be near unity.

Table 8. Morphological and thermal properties of the metal foam

Cell size (μm)	1200
Strut hydraulic diameter (μm)	100
Density (kg/m^3)	7000
Foam porosity (-)	0.92
Specific heat capacity at room temperature ($\text{kJ}/\text{K.kmol}$)	460
Thermal conductivity at room temperature	15

(W/K.m)	
---------	--

From the CFD results obtained, the performance of pellet and foam beds can be compared from different aspects. The most important aspect is the rate of heat transfer. A comparison of gas temperature profiles along the bed height for the pellet and foam beds (Figure 8) shows that the foam substrate facilitates the heat transfer from the bed wall to the bulk of the catalytic bed.

The gas temperature at the outlet of the foam bed was about 1053°C, compared to about 1005 °C for the pellet bed. As a result, a higher conversion of methane to hydrogen was obtained with catalyzed foam. Methane mole fractions at the bed exit for the pellet and foam beds were 11% and 8%, respectively (Figure 9) and the corresponding values for hydrogen mole fractions were 39% and 45% (Figure 10). It should be noted that this increased conversion is a valid but theoretical advantage, as it assumes that the tube material can stand higher temperature. In practice, the real benefit to the system translates into potential for lowering the tube wall temperature to a significant degree. This subject is studied in the following section.

Xu and Froment (1989) reported a pressure drop of about 2.5 bars for the pellet bed. It should be also noted that today SMR units are designed for lower pressure drop, in the order of 1 bar. The pressure drop for the foam bed is not only a function of the foam pore size, but also to a greater extent depends on the hydraulic diameter of the foam struts. The thickness of the struts depends on the alloy manufacturing and washcoating process. Given the virtual nature of the foam bed simulation, there is uncertainty and a lack of statistical data on how much the thickness of the washcoat will be. In this work, it was assumed that the washcoat layer would increase the strut diameter by 30 micron (from 70 microns for uncoated foam to 100 microns for washcoated foam). With this assumption, 1.05 bar foam bed pressure drop was calculated. This indicates that the use of foam as far as pressure drop is concerned is comparable to pellets. However, advanced washcoating techniques are developed that can reduce the washcoat thickness by one order of magnitude. Therefore, the use of foam can ultimately be advantageous with respect to pressure drop as well. Finally, a larger foam pore size can reduce the pressure drop significantly but at the same time will diminish the rate of mixing and heat transfer in the bed.

Figure 11 shows the radial temperature profiles for pellet and foam beds at 2, 6 and 10 m distance from the bed inlet. It can be observed that the pellet bed exhibits a significant difference in gas and solid temperatures in the vicinity of the wall. This effect seemed to be more noticeable farther from the inlet. This effect was found to be in agreement with results obtained by Taşkin (2008) from a 3-D model of highly resolved discrete cylindrical pellets in a short section of a packed tube. The author noticed that the solid phase temperatures lie some 10-20 °C lower than the fluid phase ones, due to the heat sinks caused by endothermic reaction in the solid particles. In the radial profiles presented by the author, the temperature difference is larger near the wall (typically around 20-30 °C) and has a decreasing trend moving away from the wall.

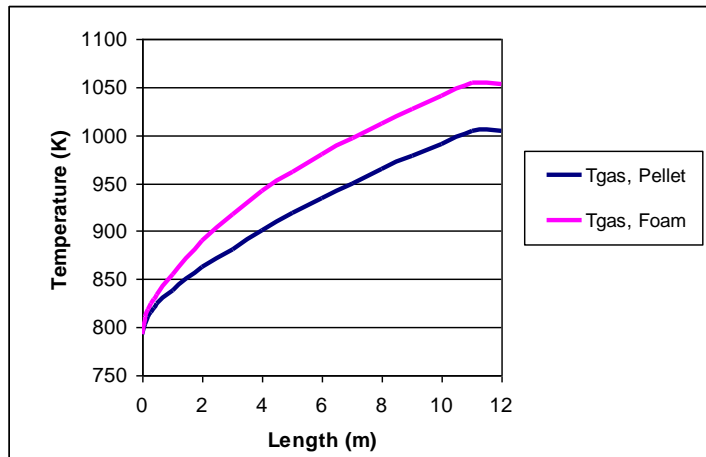


Figure 8. Comparison between axial gas beds temperature profiles for pellet and foam beds

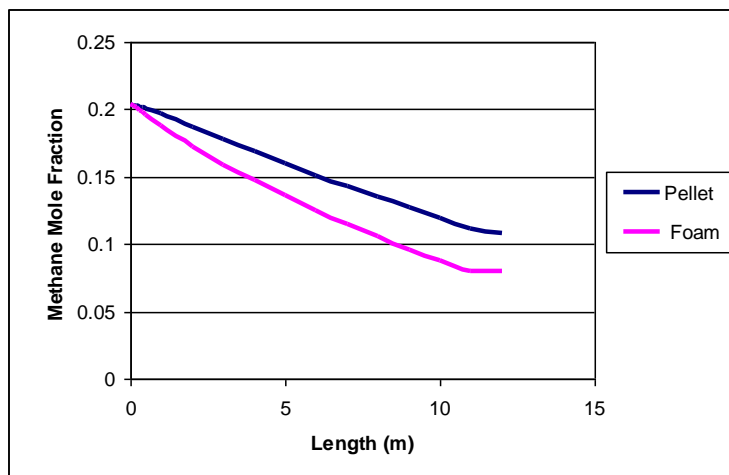


Figure 9. Axial methane mole fraction profiles for pellet and foam beds

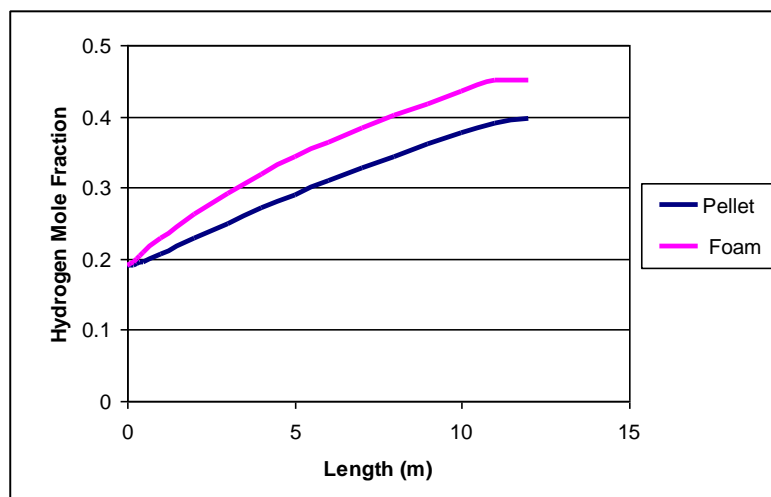


Figure 10. Axial hydrogen mole fraction profiles for pellet and foam beds

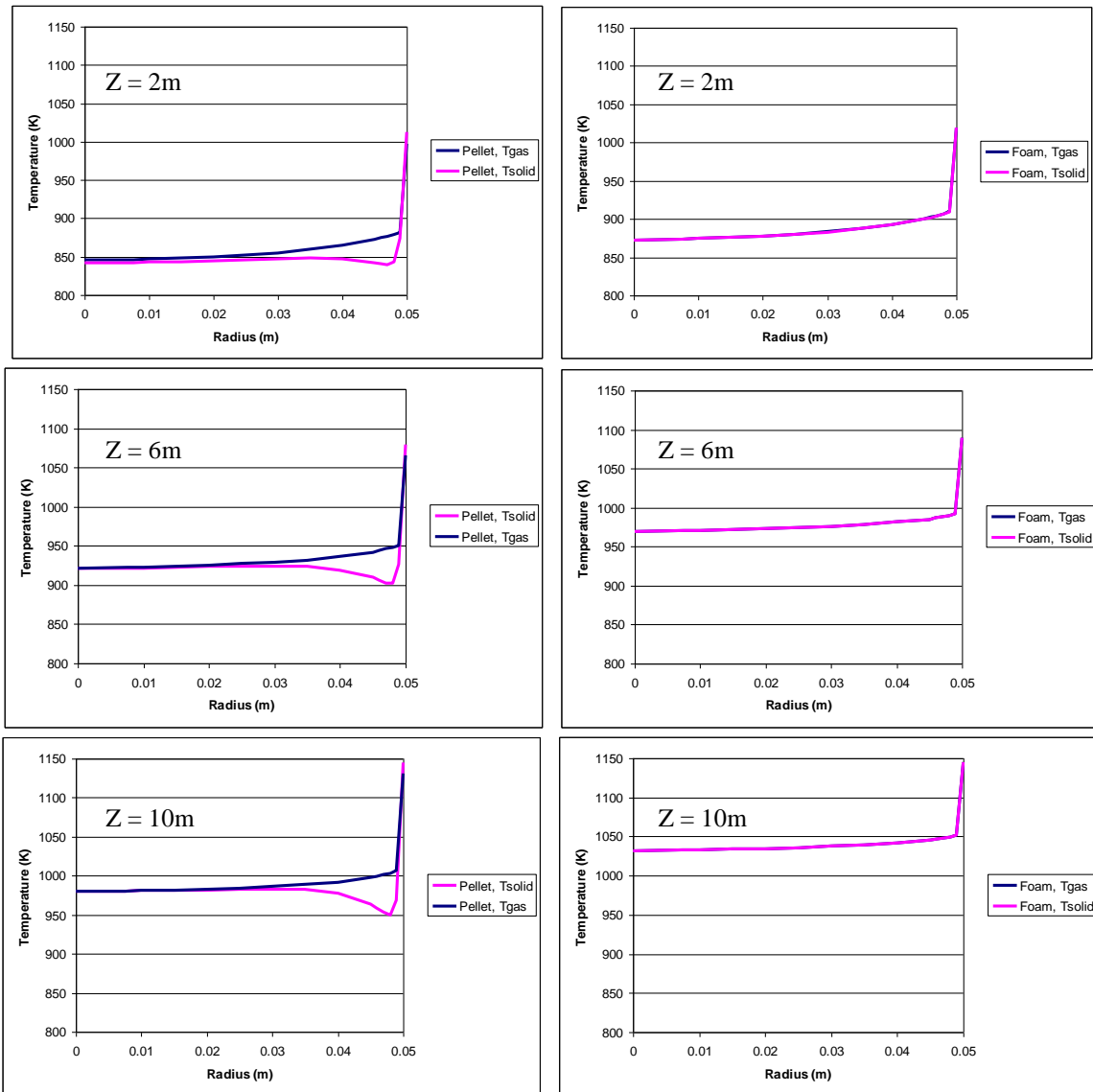


Figure 11. Comparison between radial gas and solid temperature profiles for pellet and foam beds at different bed lengths

Reduced Wall Temperature Scenario

In order to evaluate to what extent foam bed wall temperature can be reduced while maintaining the same performance as the pellet bed, several simulation trials were performed. A wall temperature profile that could fulfill the above criteria is illustrated in Figure 12 along with the original profile. In this modified profile, the wall temperature at around 3m from the inlet reaches 1033 K and is kept constant for the remaining length of the reactor. This means that the tube maximum temperature is lowered by 117 degrees from the original conditions.

A simulation run with foam catalyst under these conditions showed that the gas temperature and hydrogen mass flow rate are comparable with those obtained with the pellet bed. Therefore, there is a great potential for increasing the reactor tube life without losing productivity. Table 9 gives a summary of the results.

Increased Flowrate Scenario

Another set of “virtual” experiments were run by increasing the gas flow rate by 10% and 20% higher than the normal operating conditions, while maintaining the

reduced wall temperature as described above. Under these conditions, the foam could still provide sufficient heat such that outlet gas temperature could reach values only a few degrees lower than the one with the base flow rate. Therefore, increases in hydrogen throughput were observed. It is also interesting to note that using catalyzed foam with reduced wall temperature was shown to result in a significant decrease in wall heat flux (Table 9).

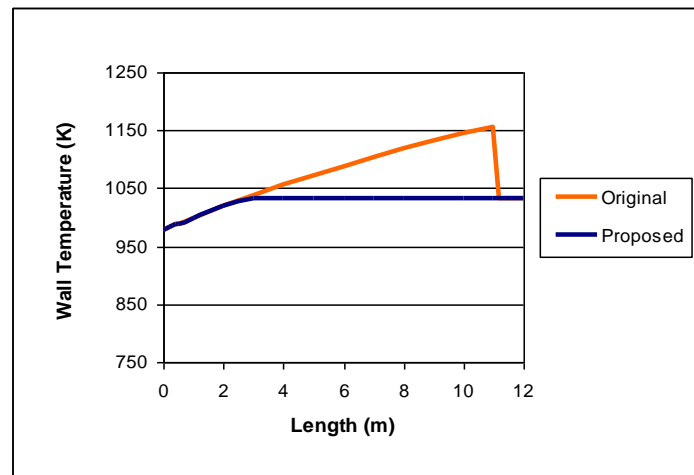


Figure 12. The original and modified wall temperature profiles for foam bed

Table 9. The effect of wall temperature profile and flow rate on foam bed performance

	Pellet	Foam			
Maximum wall temperature (K)	1150	1150	1033	1033	1033
Flow rate compared to base case (%)	100	100	100	110	120
Gas temperature, in (K)	793.1	793.1	793.1	793.1	793.1
Gas temperature, out (K)	1005	1053	1002	999	995
Methane conversion (%)	47	61	47	46	44
Hydrogen mole percent (%)	39.6	45.0	39.6	39.1	38.6
Hydrogen mass flow rate (kg/hr) per tube	16.35	22.37	16.35	18.08	19.38
Wall heat flux (kW/m ²)	85	94	67	71	76

Conclusions

A CFD model was developed for a tubular SMR reactor with pellet and foam catalysts. The pellet model was validated against operating conditions and process data provided by Xu and Froment. The model was used to study the potential advantages of catalyzed metal foam substrates as a replacement for pellets. It was demonstrated that by using foam, the tube wall temperature could be reduced by about 100 °C. This means a significantly longer tube life, and large cost savings on tube replacement. It was also shown that the foam bed was capable of processing significantly more feed than the pellet bed while using less fuel.

The results demonstrated the high potential of metal foams as catalyst substrate in chemical processes such as highly endothermic or exothermic packed bed

reactors, and other unit operations where heat and mass transfer rates control the overall system performance.

One important conclusion that can be drawn from this work is that the existing SMR units can be retrofitted with catalyzed foam and adjusted burners to introduce the above benefits and reduce the energy footprint of the unit. At the same time, new SMR units can be built with more compact designs by taking advantage of the high heat and mass transfer rates provided by metal foam substrates.

Nomenclature

Variable	Definition	Unit
A_1, A_2, A_3	Frequency factor of reaction 1,2 and 3	same dimension as k_1, k_2 and k_3
$A_{CO}, A_{H_2}, A_{H_2O}, A_{CH_4}$	Frequency factor of adsorption constant	
C_p	Heat capacity at constant pressure	J/kg.K
$D_{i,eff}$	Diffusion coefficient for species i in the mixture	m^2/s
E_1, E_2, E_3	Activation of energy of reactions 1, 2 and 3	kJ/kmol
$\Delta H_{CO}, \Delta H_{H_2}, \Delta H_{H_2O}, \Delta H_{CH_4}$	Enthalpy change of adsorption	kJ/kmol
ΔH_r	Heat of reaction	kJ/kmol
h	Enthalpy	J
h_{sg}	Solid-gas heat transfer coefficient	$W/m^2.K$
K_1, K_3	Equilibrium constant of reaction 1 and 3	bar^2
K_2	Equilibrium constant of reaction 2	-
P	Pressure	bar
$P_{CH_4}, P_{H_2O}, P_{H_2}, P_{CO_2}, P_{CO}$	Partial pressure of CH_4, H_2O, H_2, CO_2 and CO	bar
$K_{CH_4}, K_{CO}, K_{H_2}$	Adsorption constant for CH_4, CO and H_2	bar^{-1}
K_{H_2O}	Dissociative adsorption constant of H_2O	-
K_{loss}	Empirical loss coefficient in Forcheimer's equation	m^{-1}
K_{perm}	Permeability in Forcheimer's equation	m^2
k_1, k_3	Rate coefficient of reactions 1 and 3	$kmol.bar^{1/2}/kg \text{ cat.hr}$
k_2	Rate coefficient of reactions 2	$kmol/kg \text{ cat.hr.bar}$
r_1, r_2, r_3	Rates of reaction of reactions 1, 2 and 3	$kmol / kg \text{ cat.hr.bar}$
S_i	Reaction source term	$kg/m^3.s$
S_M	Momentum source term	
T	Temperature	K
U_i	Velocity components in 3 directions x, y and z	m/s
$ U $	Velocity magnitude	m/s
Y_i	Species mass fraction	-
α	Bed void fraction	-
ρ	Density	kg/m^3
λ	Thermal conductivity	$W/m.K$
μ	Dynamic viscosity	Pa. s

References

1. De Jong M., Reinders A.H.M., Kok J.B.W., Westendrop G., "Optimizing a steam-methane reformer for hydrogen production", *International Journal of Hydrogen Energy* 34 (2009), pp285-292
2. Dixon A. G., Taskin M. E., Stitt E. H., and Nijemeisland M., "3D CFD simulations of steam reforming with resolved intraparticle reaction and gradients," *Chem Eng Sci*, vol. 62, (2007), pp. 4963-4966.
3. El-Bousiffia M.A., Gunn D.J., "A dynamic Study of stem-methane reforming" *International Journal of Heat and Mass Transfer* 50 (2007) 723-733
4. Ferreira R. M. Q., Marques M. M., Babo M. F., Rodrigues A. E., "Modelling of the methane steam reforming reactor with large-pore catalysts", *Chemical Engineering Science*, Vol 47, NO 9-11 (1992), pp 2909-2914
5. Giani L., Groppi G., Tronconi E., "Mass transfer characterization of metallic foams as supports for structured catalysts", *Ind. Eng. Chem. Res.* (2005), 44, 4993-5002
6. Giani L., Groppi G., Tronconi E., "Heat transfer characterization of metallic foams", *Ind. Eng. Chem. Res.* (2005), 44, 9078-9085
7. Grenvskott S., Rusten T., Hillestad M., Edwin E., Olsvik O., "Modelling and simulation of a steam reforming tube with furnace", *Chemical Engineering Science* 56 (2001), 597-603
8. Hyman M.H., "Simulate methane reformer reactions", *Hydrocarbon Processing* Vol 47, No 7 (1968), pp131-137
9. Kirillov V.A., Kuzin N.A., Kulikov A.V., Fadeev S.I., Shigarov A.B., Sobyenin V.A., "Thermally coupled catalysis reactor for steam reforming of methane and liquid hydrocarbons: Experimental and mathematical modelling", *Theoretical Foundation of Chemical Engineering*, Vol 37, No 3 (2003), pp 276-284
10. Kvamsdal H.M., Svendsen H.F., Hertzberg T., Olsvik O., "Dynamic simulation and optimization of a catalytic steam reformer", *Chemical Engineering Science* 54 (1999), 2697-2706
11. Lu W., Zhao C.Y., Tassou S.A., "Thermal analysis on metal-foam filled heat exchanger. Part 1. Metal-foam filled pipes", *International Journal of Heat and Mass Transfer* 49 (2006) 2751-2761
12. Mohammad Taghi Sadeghi, Mazaher Molaei, "CFD simulation of a methane steam reforming reactor", *International Journal of Chemical Reactor Engineering* Vol6 (2008), Article A50
13. Pedernera M. N., Pina J., Borio D. O., Bucala V., "Use of heterogeneous two-dimensional model to improve the primary steam reformance" *Chemical Engineering Journal* 94 (2003) 29-40
14. Peters, P.E., Schifano, R.S. AND Harriott, P., *Heat Transfer in Packed-Tube Reactors*. *Industrial & Engineering Chemistry Research*, 27 (1988), 226-233.
15. Taşkin E., "CFD simulation of transport and reaction in cylindrical catalyst particles", Ph.D. Dissertation, Worcester Polytechnic Institute (2008)
16. Twigg M. V., Richardson J., "Fundamental and applications of structured ceramic foam catalysts", *Ind. Eng. Chem. Res.* (2007), 46, 4166-4177
17. Twigg M. V., Richardson J., "Theory and application of ceramic foam catalysts", *Trans IChemE*, (2002) Vol 80, Part A,
18. Walther G., Kloden B., Buttner T., Weissgarber T., Kieback B., Bohm A., Naumann D., Saberi S., Timberg L., "A New Class of High Temperature and Corrosion Resistant Nickel-Based Open-Cell Foams", *Advanced Engineering Materials* (2008), 10 (9), 803-811

19. Zhao C. Y., Kim T., Lu T.J. and Hodson H. P., "Thermal Transport Phenomena in Porvair Metal Foams and Sintered Beds", Final Report, Department of Engineering University of Cambridge (2001).
20. Zhao C.Y., Lu T.J., Hodson H.P., "Thermal radiation in ultralight metal foams with open cells", *International Journal of Heat and Mass Transfer* 48 (2004) 2927-2439
21. Zhao C.Y., Lu T. J., Hodson H.P., "Natural convection in metal foams with open cells", *International journal of heat and mass transfer* 48 (2005) 2452-2463
22. Xu J., Froment G. F., "Methane Steam Reforming, Methanation and Water-Gas Shift: I. Intrinsic Kinetics", *AIChE Journal*, January, (1989) Vol. 35, No. 1, pp 88-96.
23. Xu J., Froment G. F., "Methane Steam Reforming: II. Diffusional Limitations and Reactor Simulation", *AIChE Journal*, January, (1989) Vol. 35, No. 1, pp 97-103.